British Journal of Pharmacology (2004) 142, 305–316
www.nature.com/bjp

Differential regulation of calcium homeostasis in adenocarcinoma cell line A549 and its Taxol-resistant subclone

[1]Shanthala Padar, [2]Cornelis van Breemen, [1]David W. Thomas, [3]James A. Uchizono, [1]John C. Livesey & *,[1]Roshanak Rahimian

[1]Department of Physiology & Pharmacology, Thomas J. Long School of Pharmacy and Health Sciences, University of the Pacific, Stockton, CA 95211, U.S.A.; [2]BC Research Institute for Children's and Women's Health, University of British Columbia, Vancouver, Canada V6H3V4 and [3]Department of Pharmaceutics and Medicinal Chemistry, Thomas J. Long School of Pharmacy and Health Sciences, University of the Pacific, Stockton, CA 95211, U.S.A.

1 Drug resistance is a fundamental problem in cancer chemotherapy. Intracellular calcium concentration ($[Ca^{2+}]_i$) may play a role in the development of chemoresistance. We investigated the regulatory role of $[Ca^{2+}]_i$ in Taxol resistance in the non-small-cell lung cancer cell line A549 and its chemoresistant subclone A549-T24.

2 Measurement of cytosolic calcium ($[Ca^{2+}]_c$) in single cells and cell populations revealed similar levels of basal calcium in the two cell lines. However, a reduced response to thapsigargin (a sarcoplasmic/endoplasmic reticulum Ca^{2+}-ATPase (SERCA) inhibitor) in A549-T24 cells compared to the parent cell line suggested a lower ER Ca^{2+} content in these cells.

3 mRNA expression of SERCA2b and SERCA3, major Ca^{2+} pumps involved in ER Ca^{2+} homeostasis, did not significantly differ between the two cell lines, as revealed by RT–PCR.

4 An altered calcium influx pathway in the Taxol-resistant cell line was observed. Modulation of the ER calcium pools using CMC (4-chloro-*m*-cresol) and ATP revealed lower ryanodine receptor (RyR) and IP_3 receptor (IP_3R)-sensitive Ca^{2+} stores in the chemoresistant cell line.

5 Western blot and RT–PCR studies suggested that A549-T24 cells expressed higher levels of the antiapoptotic protein Bcl-2 and the calcium-binding protein sorcin, respectively, in comparison to the parent cell line. Both of these proteins have been previously implicated in chemoresistance, in part, due to their ability to modulate $[Ca^{2+}]_i$.

6 These results suggest that altered intracellular calcium homeostasis may contribute to the Taxol-resistant phenotype.

British Journal of Pharmacology (2004) **142,** 305–316. doi:10.1038/sj.bjp.0705755

Keywords: Apoptosis; calcium; endoplasmic reticulum; sorcin; chemoresistance; taxol

Abbreviations: $[Ca^{2+}]_c$, cytosolic Ca^{2+}; $[Ca^{2+}]_{er}$, endoplasmic reticulum Ca^{2+}; $[Ca^{2+}]_i$, intracellular calcium; $[Ca^{2+}]_o$, extracellular Ca^{2+}; CCE, capacitative calcium entry; CMC, 4-chloro-*m*-cresol; ER, endoplasmic reticulum; IP_3R, inositol 1,4,5-triphosphate receptor; RyR, ryanodine receptor; SERCA, sarcoplasmic/endoplasmic reticulum Ca^{2+}-ATPase; SOC, store-operated channel; TG, thapsigargin

Introduction

Taxol® (paclitaxel), a microtubule inhibitor, is one of the most effective chemotherapeutic agents against various tumors. The mechanism of anticancer action of Taxol involves mitotic arrest of the cells due to microtubule stabilization, eventually resulting in apoptosis (Blagosklonny & Fojo, 1999; Miller & Ojima, 2001). The emergence of chemoresistance is a major obstacle in Taxol treatment. A common mechanism of resistance to chemotherapy is the overexpression of plasma membrane drug efflux proteins called P-glycoproteins (P-gp). However, inhibition of these pumps does not always result in the reversal of chemoresistance in patients (Ferry *et al*., 1996). In fact, a multitude of survival signaling pathways are activated during the development of chemoresistance.

Calcium, an early-response second messenger, plays a key role in a number of physiological processes including cell proliferation, differentiation and apoptosis (van Breemen & Saida, 1989; Berridge *et al*., 2000). Intracellular calcium levels are maintained by the coordinated actions of various calcium pumps, ion channels and calcium-buffering proteins such as calreticulin, calsequestrin and sorcin. Cytosolic calcium ($[Ca^{2+}]_c$) levels in nonexcitable cells are typically increased by one or both of the following mechanisms: (1) Ca^{2+} release from the intracellular stores contained in the endoplasmic reticulum (ER) and (2) Ca^{2+} influx through plasma membrane channels such as store-operated channels (SOC), voltage-gated calcium channels (VGCC) and receptor-operated channels (ROC). While the controlled increase in intracellular Ca^{2+} concentration ($[Ca^{2+}]_i$) is indispensable to normal cellular processes, excessive and uncontrolled $[Ca^{2+}]_i$ can be lethal as it can result in apoptosis (Trump & Berezesky, 1995; McConkey, 1996). In fact, the cytotoxic effect of a number of anticancer agents is coupled to cellular calcium overload (Marin *et al*., 1996). In support of this evidence, buffering of intracellular

*Author for correspondence; E-mail: rrahimian@pacific.edu
Advance online publication: 5 April 2004

Ca^{2+} with BAPTA-AM (acetoxymethyl)-1,2-bis(*o*-aminophenoxy)ethane-*N,N,N′,N′*-tetraacetic acid) (Lynch *et al*., 2000; Kalivendi *et al*., 2001; Mandic *et al*., 2002) or removal of extracellular Ca^{2+} with EGTA protected cells from apoptosis (McConkey *et al*., 1989). Chen *et al*., 2002 showed that resistance to thapsigargin (TG) (an inhibitor of sarcoplasmic/endoplasmic reticulum Ca^{2+}-ATPase (SERCA)) mediated apoptosis is associated with reduced intracellular Ca^{2+} pools in doxorubicin-resistant MCF-1/DOX cells. Furthermore, a significant decrease in $[Ca^{2+}]_i$ was observed in doxorubicin-resistant MCF-7/DOX cells (Mestdagh *et al*., 1994) and cisplatin-resistant $A549_{CDDP}$ cells (Liang & Huang, 2000) compared to their parent cell lines. In contrast, a number of researchers (Tsuruo *et al*., 1984; Nygren *et al*., 1991) reported an elevated $[Ca^{2+}]_i$ in a multidrug-resistant lung cancer cell line.

Sorcin, a 22 kDa calcium-binding protein (Valdivia, 1998; Maki *et al*., 2002), has been shown to be upregulated in several P-gp-expressing lymphocytes or drug-resistant tumor cells (Witkowski & Miller, 1999). Sorcin overexpression is associated with poor outcome in leukemia patients (Li *et al*., 2002; Tan *et al*., 2003). Increased sorcin expression by gene transfer rendered ovarian and breast cancer cells resistant to Taxol (Parekh *et al*., 2002). The precise mechanism of action of sorcin in the development of chemoresistance, however, is not known.

The main aim of the present study was to characterize the alterations in the regulatory pathways of cellular calcium handling and their possible role in the development of chemoresistance. We used the human lung adenocarcinoma cell line A549 and its Taxol-resistant subclone A549-T24 to explore the relative contributions to these alterations in the various components of calcium homeostasis such as SOC or ROC, SERCA and calcium pools. In addition, we measured the expression of Bcl-2 and sorcin, two known modulators of $[Ca^{2+}]_c$.

Methods

Cell culture and reagents

The lung adenocarcinoma cell line A549 (ATCC CCL-185) and its Taxol-resistant subclone A549-T24 (generously provided by Dr Susan Horwitz, Albert Einstein College of Medicine, New York) were cultured as monolayers in DMEM-F12 media supplemented with 10% FBS, penicillin (100 U ml^{-1}), streptomycin (100 $\mu g\,ml^{-1}$) and 1% L-glutamine, in a humid atmosphere at 37°C with 95% air and 5% CO_2. To maintain the drug resistance phenotype, 24 nM of Taxol was added to the media of A549-T24 cells during routine subculturing. All the cell culture reagents, Taxol, TG, $NiCl_2$, $CaCl_2$ and ATP were purchased from Sigma Chemical Co. (St Louis, MO, U.S.A.). Calcein-AM, propidium iodide and Fura-2 AM was obtained from Molecular Probes (Eugene, OR, U.S.A.). SK&F96365 was obtained from Biomol (Plymouth Meeting, PA, U.S.A.). Stock solutions of Taxol (1 mM in DMSO), TG (1 mM in DMSO), 4-chloro-*m*-cresol (CMC; 50 mM in ethanol), ATP (100 mM) and SK&F96365 (50 mM) were stored at −20°C. Stock solutions of $CaCl_2$ (1 M), $BaCl_2$ (1 M) and $NiCl_2$ (1 M) were stored at room temperature. All the stock solutions were prepared in water, unless mentioned otherwise.

Cell viability (MTS) assay

The extent of cell viability after Taxol treatment was measured using the MTS assay (Promega, Madison, WI, U.S.A.). The cells were seeded (3×10^3 cells/100 μl per well) in 96-well tissue culture plates and allowed to attach overnight. They were then treated with various concentrations of Taxol for 48 h. At the end of the treatment period, the media was replaced with fresh complete media containing MTS reagent for 1 h. The absorbance of the reduced dye was measured at 490 nm using a 96-well plate reader (Thermomax, Molecular Devices, Sunnyvale, CA, U.S.A.). The cell viability was expressed as the percent of survival of the control.

Detection of Apoptosis

(a) Calcein-AM and propidium iodide assay Taxol-induced apoptosis was detected by double labeling with Calcein-AM and propidium iodide. The cells were seeded at a density of 3×10^5 in six-well plates and allowed to attach overnight. Following 48 h Taxol treatment, the media was removed and the cells were rinsed with PBS. To visualize the living and apoptotic cells, they were loaded directly in the six-well plates at room temperature with 1.5 μM Calcein-AM (Molecular Probes, Eugene, OR, U.S.A.) in PBS for 15 min, followed by 3 $\mu g\,ml^{-1}$ propidium iodide in PBS for another 10 min. After rinsing twice with PBS to remove excess dye, fluorescence emitted by Calcein-AM (green) and propidium iodide (red) was visualized by fluorescence microscopy (Nikon Inc., Melville, NY, U.S.A.) using appropriate filters.

(b) Caspase-3 assay Caspase-3-like protease activity was measured by detecting the cleavage of the cell-permeable fluorogenic peptide substrate DEVD-AMC using the Apo-Alert CPP32/caspase-3 assay kit (Clontech, Palo Alto, CA, U.S.A.). Briefly, 2×10^6 exponentially growing cells were treated with vehicle or Taxol at the indicated concentration. Cells were harvested at 48 h and pelleted by centrifugation. Cell pellets were lysed in lysis buffer (50 μl) and the lysate was incubated on ice for 10 min before centrifugation (18,300 × *g*, for 3 min at 4°C). To the supernatant of each sample, 2 × reaction buffer (50 μl) supplemented with 10 mM dithiothreitol (DTT) was added and the samples were incubated at 4°C. The substrate DEVD-AMC was added to all tubes (5 μl, 50 μM), and the samples were incubated for 1 h at 37°C. The release of AMC was measured (excitation at 360 ± 19 nm; emission at 460 ± 17 nm) using a fluorescence spectrophotometer (PTI, NJ, U.S.A.). Caspase-3 activity was reported as fold increase compared to the drug-free control.

Intracellular free calcium measurements

The cells grown on poly-L-lysine or collagen IV-coated glass coverslips were rinsed twice with Hank's buffered salt solution (HBSS) (20 mM HEPES, 10 mM glucose, 150 mM NaCl, 1.2 mM $CaCl_2$, 5 mM KCl, 1 mM $MgCl_2$, pH 7.4). They were then loaded with 1 ml of 1.5 μM Fura-2 AM dissolved in HBSS from a stock solution of 1.5 mM in DMSO containing 20% pluronic acid F-127, at room temperature for 30 min and subsequently rinsed twice with HBSS. Next, the cells were incubated in HBSS for an additional 30 min to allow complete de-esterification of the dye.

The average fluorescence of a whole population of Fura-2 AM-loaded cells was measured by using continuous rapid alternating excitation from monochromators (340 and 380 nm) and emission at 510 nm in a fluorescence spectrophotometer equipped with a xenon lamp (PTI, NJ, U.S.A.). The fluorescence ratio was recorded every 0.1 s using Felix Fluorescence Analysis Software.

To measure the fluorescence intensity in individual cells, the coverslips were mounted on the stage of a Nikon Diaphot inverted microscope. About 15–20 cells were randomly chosen for fluorescence imaging. Fluorescent images were obtained by alternate excitation at 340 and 380 nm (bandwidth 10 nM) ultraviolet light and the emission signal at 510 nm (bandwidth 40 nm) was collected using an ICCD camera (Cohu, 4810 series). Fluorescence was recorded every 3 s as digital images using Northern Eclipse software by Empix Imaging Systems. The readings were reported as a 340/380 fluorescence ratio. $[Ca^{2+}]_i$ can be calculated using the equation of Grynkiewicz *et al.* (1985), as $[Ca^{2+}]_i = K_d b[(R-R_{min})/(R_{max}-R)]$, where K_d is the dissociation constant of the Ca^{2+}-Fura 2 complex; R is the above-mentioned fluorescence ratio (F_{340}/F_{380}); R_{min} and R_{max} are the ratios measured by the addition of the Ca^{2+} ionophore ionomycin (10 μM) to Ca^{2+}-free (with 10 mM ethylene glycol-bis(β-aminoethyl ether)-*N*,*N*,*N*′,*N*′-tetraacetic acid (EGTA)) solution and Ca^{2+}-replete (2 mM $CaCl_2$) solution, respectively; and b is the ratio of the 380 nm signals in Ca^{2+}-free and Ca^{2+}-replete solution. Using a $K_d = 224$ nM, $R_{min} = 0.718$, $R_{max} = 6.3$ and $b = 5.4$, the resting Ca^{2+} level for A549 was estimated at about 62 nM. Using a $K_d = 224$ nM, $R_{min} = 0.702$, $R_{max} = 7.15$ and $b = 6$, the resting Ca^{2+} level for A549-T24 was estimated at about 67 nM. In some experiments, the cells were pretreated with IC_{50} concentrations of Taxol for 24 h.

Semi-quantitative RT–PCR

All reagents for RT–PCR were purchased from Qiagen Inc (Valencia, CA, U.S.A.) unless mentioned otherwise. The cells were harvested using 0.25% trypsin and centrifuged at 1000 r.p.m. The pellet was subsequently washed twice with ice-cold PBS. Total RNA was isolated using RNeasy RNA isolation kit according to the manufacturer's instructions. First-strand cDNA was synthesized by reverse transcription of 1 μg of total RNA using Sensiscript reverse transcriptase in a volume of 20 μl at 47°C for 60 min. The gene fragments were specifically amplified using HotStar *Taq* polymerase. Internal variations were normalized using 18S rRNA (Ambion Inc, Austin, TX, U.S.A.). The primers for sorcin, SERCA2b, SERCA3, Trp1, Trp3 and Trp4, IP_3 receptor type1-3 and the PCR protocol were designed based on previously published data (Kawano *et al.*, 2002; Liu *et al.*, 2002; Riccio *et al.*, 2002; Tan *et al.*, 2003). The PCR products were then electrophoresed on a 2% agarose gel and stained with ethidium bromide. Densitometric analysis was performed using UNSCAN-IT gel scanner software (Silk scientific Corporation, Orem, UT, U.S.A.).

Western blot analysis

The cells were harvested and lysed in lysis buffer (20 mM Tris–HCl, pH 7.5, 150 mM NaCl, 1 mM Na_2EDTA, 1 mM EGTA, 1% Triton, 2.5 mM sodium pyrophosphate, 1 mM β-glycerophosphate, 1 mM Na_3VO_4, 1 μg ml^{-1} leupeptin, 1 mM PMSF). The lysate was boiled at 90°C for 5 min. In all, 25 μg of proteins were analyzed by 12% SDS–polyacrylamide gel electrophoresis. Proteins were then transferred to a nitrocellulose membrane and incubated in blocking buffer (5% nonfat dry milk in PBS) for 2 h before incubation with mouse anti-bcl-2 polyclonal antibody (SantaCruz Biotechnology, Santa Cruz, CA, U.S.A; 1:200 dilution) at 4°C for overnight. Subsequently, the blots were probed with peroxidase conjugated anti-mouse antibody (1:1000 dilution) for 2 h and the proteins were detected by ECL (Pierce, Rockford, IL, U.S.A).

Statistical analysis

The traces are representative of similar responses obtained in at least six preparations (unless specifically noted). All values reported are mean ± sample standard deviation (s.d.), and the Student's *t*-test was used to compare groups. Chemicals and/or drugs were applied as indicated by the horizontal bars or arrows in each figure.

Area under the curve

The area under the curve (AUC) of the ratio curve was determined by applying the trapezoidal method on the original data. Depending on the comparison being made, the AUC integration bounds contained either 150 or 200 s, but the length of integration was the same for each matched up experimental comparison. The data were normalized prior to the AUC calculation by subtracting the average baseline value. Two-tailed, Mann–Whitney rank sum statistics were used to determine the statistical significance for each comparison; *P*-values were reported and *P*-values equal to or less than 0.05 for Type I errors were considered significant. Statistical power (or Type II error) was difficult to determine for this non-parametric statistic and was, therefore, not reported.

Slope calculations

All slope calculations were determined from box-car convolved, smoothed data. The original data were smoothed using a symmetric, uniform-weighted, moving convolved box-car function; this smoothing eliminated the high frequency noise in the original signal. In the TG/Ba^{2+} and the ATP slope calculations, the box-car convolution contained the seven preceding, seven proceeding, and the middle data point. Equally weighted linear regression was performed and the average slope ± sample standard deviation was reported for each group. The statistical significance was determined by the conservative, non-parametric Mann–Whitney rank-sum statistic – 3–7 per group. The Type I error cutoff for statistical significance was 0.05 and statistical power was not calculated. The first 30 and 60 s of data in the ATP experiments and TG/Ba^{2+} experiments, respectively, were used in the linear regression.

Estimations of the Ca^{2+} efflux slopes (in TG/0Ca^{2+}/EGTA experiments) were calculated from the smoothed data, but not with linear regression – due to the small number of data points between the pre- and post-EGTA steady-state plateaus. The slope was calculated by taking the difference between the average steady-state plateaus (i.e. pre-EGTA plateau minus post-EGTA plateau) and dividing by the time difference; the

mean ± sample standard deviation was reported. The large number of experiments per group (A549, $N = 19$; T24, $N = 15$) supported the use of a Student's *t*-test to determine statistical significance.

Results

Determination of IC_{50} of Taxol

Previous studies have shown that the drug-resistant subclone A549-T24, established by stepwise treatment with increasing Taxol concentrations, is resistant to up to 24 nM Taxol (Torres & Horwitz, 1998). In the present study, we treated cells with various concentrations of Taxol for 48 h and measured cell viability by the MTS assay. As shown in Figure 1a and b, a 10-fold difference in the IC_{50} value was found between the cell lines ($P < 0.01$, $N = 3$).

Taxol induces apoptosis

Taxol has been shown to induce cell cycle arrest and apoptosis depending on the cell type. To understand the mechanism of Taxol-induced cytotoxicity in our experimental models, we analyzed the cells with the Calcein-AM and propidium iodide double-staining technique. Calcein-AM is a highly hydrophobic, nonfluorescent dye that rapidly diffuses through the plasma membrane. Once inside the cell, it is cleaved by esterases releasing fluorescent hydrophilic calcein that becomes trapped inside. Propidium iodide, on the other hand, enters the cell only when the membrane integrity is compromised. A positive staining for propidium iodide is indicative of apoptosis. Our results (Figure 2) suggest that both A549 and A549-T24 cells underwent apoptosis when treated with IC_{50} concentrations of Taxol. However, the sensitivity of A549-T24 to Taxol-mediated apoptosis is at least 10 times lower compared to the parent cell line ($N = 3$). In addition, caspase-3 activity was used to quantify the cell apoptotic response to Taxol treatment. In A549-T24, caspase-3 activity was significantly elevated relative to drug-free control cultures in A549 and A549-T24 by treatment with Taxol for 48 h (2.5 ± 0.4 and 2.9 ± 0.3-fold, respectively; $P < 0.01$, $N = 3$).

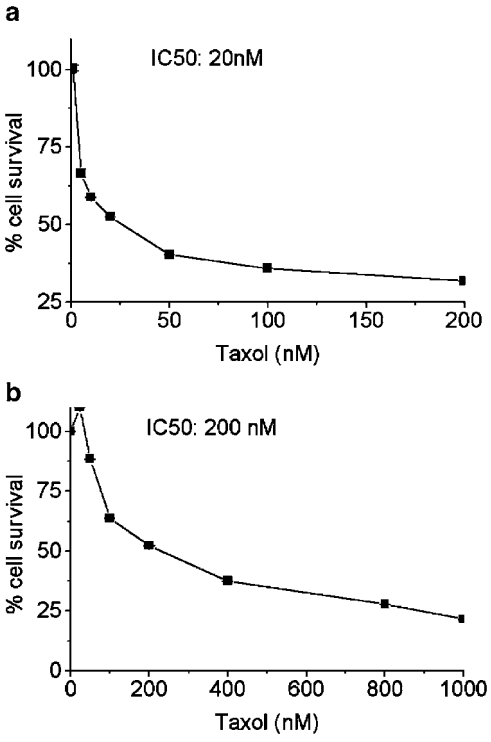

Figure 1 Taxol induced cytotoxicity in tumor cells. The cells were seeded in 96-well plates (3×10^3 per well) were treated with increasing concentrations of Taxol for 48 h. Cell viability was measured by the MTS assay as described in Methods. The values represent the mean cell survival ± deviation from three independent experiments compared with the untreated control cells (100% survival). A 10-fold difference in the IC_{50} value was found between the cell lines ($P < 0.01$, $N = 3$). (a) A549 cells, (b) A549-T24 cells.

Differential effect of TG on $[Ca^{2+}]_i$ mobilization

Several studies have shown that altered intracellular calcium can contribute to chemoresistance (Chen *et al*., 2002; Liang & Huang, 2000; Mestdagh *et al*., 1994). In order to determine whether that is the case in our experimental model, we loaded cells with Fura-2 AM and $[Ca^{2+}]_c$ was measured. Basal $[Ca^{2+}]_c$ levels were not significantly different in the two cell lines. The resting Ca^{2+} levels for A549 and A549-T24 were estimated at 64.7 ± 2.5 and 68.7 ± 3.8 nM, respectively ($N = 3$, $P > 0.05$). In the presence of extracellular Ca^{2+} (1.2 mM), TG (100 nM) increased $[Ca^{2+}]_c$ in A549 (Figure 3a) and A549-T24 (Figure 3b) cells. In both the cell lines, TG treatment resulted in a rapid increase, followed by a prolonged elevation of $[Ca^{2+}]_c$. The $[Ca^{2+}]_c$ response to TG is characterized by a biphasic upstroke reaching a peak value before it declines to a plateau (plateau1 and plateau 2 in Figure 3c), which is elevated above the resting level. The extent of TG-induced $[Ca^{2+}]_c$ increase at the peak was significantly higher in A549 cells than its chemoresistant counterpart (1.8-fold, $P < 0.01$, $N = 6$). Similar results were obtained in cell population studies and

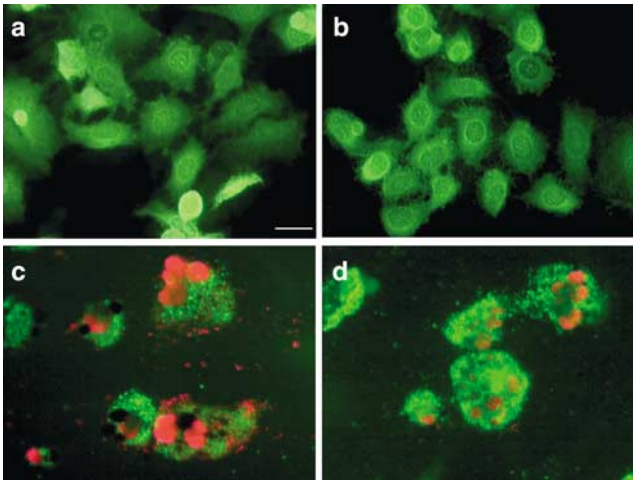

Figure 2 Fluorescent images of calcein-AM (green) and propidium iodide (red) double-stained cells. Tumor cells were grown on poly-L-lysine or Collagen IV-coated coverslips, exposed to Taxol for 48 h, and subsequently analyzed for apoptosis as described in Methods. (a) A549 control, (b) A549-T24 control, (c) A549 treated with 20 nM Taxol, (d) A549-T24 treated with 200 nM Taxol. Scale bar = 25 μm.

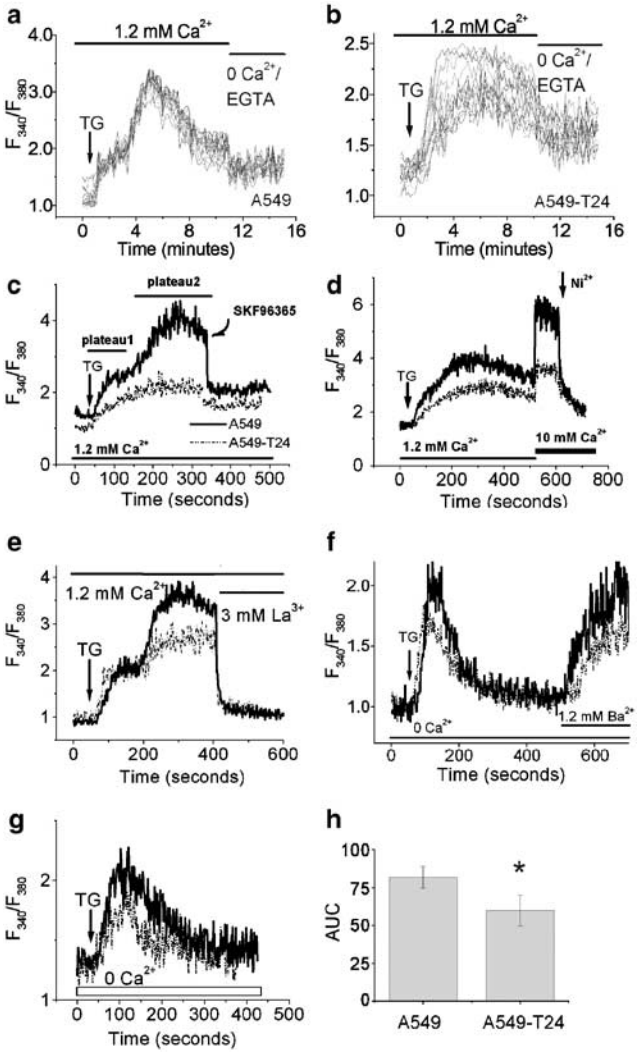

Figure 3 Steady-state and agonist-induced intracellular calcium levels in tumor cells. The cells were loaded with Fura-2 AM and $[Ca^{2+}]_c$ was detected as described in Methods. (a, b) Single-cell calcium measurements by fluorescence imaging microscopy in TG (100 nM)-treated A549 (a) and A549-T24 cells (b), followed by removal of extracellular calcium. $[Ca^{2+}]_c$ changes were recorded in 15–20 cells. (c–e) A representative tracing of the response of $[Ca^{2+}]_i$ of A549 and A549-T24 cells in response to TG (100 nM), followed by SKF96365 (50 μM) treatment (c), addition of extracellular calcium (10 mM) and Ni^{2+} (10 mM) treatment (d), or La^{3+} (3 mM) treatment (e). (f) A representative tracing of the response of $[Ca^{2+}]_i$ of A549 and A549-T24 cells in response to TG (100 nM) in Ca^{2+}-free medium, followed by addition of 1.2 mM Ba^{2+}. (g) A representative tracing of the response of $[Ca^{2+}]_i$ of A549 and A549-T24 cells in response to TG (100 nM) in the absence of extracellular calcium. (h) The mean $\pm$ s.d. of AUC of TG (100 nM) response in the absence of extracellular Ca^{2+}. *Significantly different ($P<0.01$, $N=6$) from A549 by Mann–Whitney test.

single-cell calcium measurements (Figure 3a and b vs c). Since the variability between the cells in terms of TG response within the population of each cell line was insignificant, as judged by single-cell $[Ca^{2+}]_c$ measurements, the majority of the subsequent Ca^{2+} measurements were made by fluorescence spectrophotometry of cell populations. Furthermore, in order to show that we had a comparable Fura-2 AM loading in these cell lines, we repeated the above experiments in the presence of sulfinpyrazone (200 μM), to reduce the efflux of Fura-2 AM from the cells. In fact, we found that the fluorescence intensity or ratio was similar for both cell lines in the presence or absence of sulfinpyrazone (data not shown).

As shown in Figure 3a and b, the second phase of TG-induced increase in $[Ca^{2+}]_c$ (i.e., the portion following the notch on the upstroke) was almost completely abolished by removal of extracellular calcium or by addition of an SOC blocker, SK&F96365 (50 μM) (Figure 3c). However, the $[Ca^{2+}]_c$ did not return completely to baseline after removal of extracellular Ca^{2+}. In addition, the *t*-test results revealed that the slope of Ca^{2+} decline upon removal of extracellular Ca^{2+} in the presence of TG was similar in A549 and A549-T24 (-2.27 ± 1.08 and $-1.80\pm0.98\,m^{-1}$, respectively; $P>0.1$, $df=32$, $N=15$–19). A subsequent increase in the extracellular Ca^{2+} concentration to 10 mM during the sustained influx phase led to a robust increase in $[Ca^{2+}]_c$, which was completely blocked by the nonspecific calcium channel blocker Ni^{2+} (10 mM) (Figure 3d). As shown in Figure 3d, the elevation of $[Ca^{2+}]_c$ in response to added Ca^{2+} (10 mM) was much higher in A549 cells relative to A549-T24 cells.

In addition, we performed the experiment to incapacitate SOCs with a high concentration of La^{3+}. In the presence of extracellular Ca^{2+} concentration (1.2 mM), TG (100 nM) increased $[Ca^{2+}]_c$ in A549 and A549-T24 cells. The addition of 3 mM La^{3+} returned the Ca^{2+} signals to the baseline in both cell lines (Figure 3e). However, there was no observable difference in Ca^{2+} signal decay in A549 and A549-T24 cells.

To address the possibility that the reduced Ca^{2+} response in the A549-T24 cell line was due to increased activity of Ca^{2+} extrusion mechanisms (e.g., plasma membrane Ca^{2+}-ATPase (PMCA) or Na^+/Ca^{2+} exchanger (NCX)), we examined influx responses using Ba^{2+} ions as a Ca^{2+} surrogate. Divalent ions other than Ca^{2+} serve as poor substrates for Ca^{2+}-sensitive pumps and exchangers, thereby allowing a more direct assessment of the unidirectional flow of divalent ions (Graf *et al*., 1982; Brownlow & Sage, 2003).

Experiments were carried out by adding TG (100 nM) in Ca^{2+}-free medium, followed by addition of 1.2 mM Ba^{2+} (Figure 3f). As shown in Figure 3f, the initial rate of Ba^{2+} entry was significantly greater in A549 than that seen in A549-T24 (0.00845 ± 0.00238 vs $0.00509\pm0.00127\,s^{-1}$, respectively; $P=0.05$, $N=3$).

In the absence of extracellular Ca^{2+}, TG treatment resulted in a single Ca^{2+} transient in both cell lines (Figure 3g). However, the AUC of TG induced Ca^{2+} signals in calcium-free buffer was significantly greater ($P<0.01$, $N=6$) in A549 cells in comparison to A549-T24 cells (Figure 3h).

Agonist-sensitive Ca^{2+} pools

To further explore the ER calcium pools, we stimulated these tumor cells with ATP, a purinergic receptor agonist that releases ER Ca^{2+} in an IP_3-dependent pathway. ATP (100 μM) induced Ca^{2+} release in both A549 and A549-T24 cells, suggesting the presence of functional IP_3 receptors in these cells (Figure 4a). Although both cell lines exhibited a sustained influx of Ca^{2+} upon ATP treatment (which was effectively blocked with Ni^{2+}), the rate of Ca^{2+} decay was twice as fast in A549-T24 cells in comparison to A549 cells ($P<0.01$, $N=7$). By comparing the AUC, we can conclude that ATP-mediated

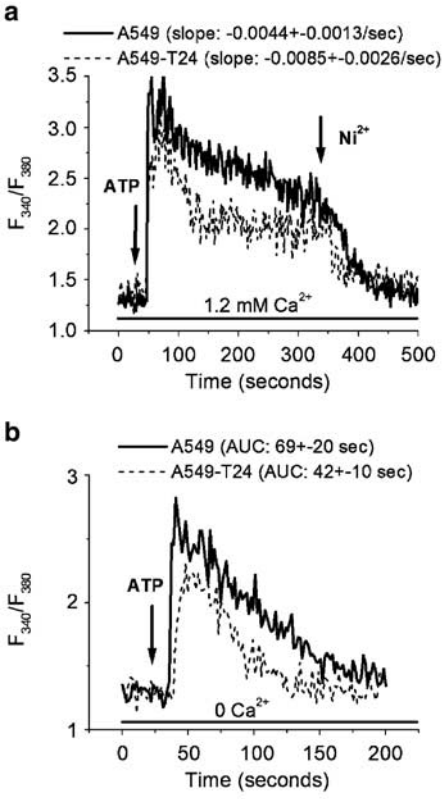

Figure 4 ATP-induced Ca^{2+} signals. A representative tracing of the response of $[Ca^{2+}]_i$ of A549 and A549-T24 cells in response to ATP (100 μM) in the presence (a) and absence (b) of 1.2 mM extracellular calcium. The rate of $[Ca^{2+}]_i$ decay upon ATP response in the presence of extracellular calcium was slower in A549 compared to A549-T24 ($P<0.01$, $N=7$). The mean $\pm$ s.d. of AUC of ATP response in the absence of extracellular calcium was significantly higher in A549 compared to A549-T24 ($P<0.01$, $N=7$).

$[Ca^{2+}]_c$ increase is significantly higher in A549 cells (Figure 4a) ($P<0.01$, $N=7$). Similar results were obtained when cells were stimulated with two other IP_3-releasing agents, bradykinin and histamine (data not shown). When the cells were stimulated with ATP in the absence of extracellular calcium ($[Ca^{2+}]_o$), the amount of Ca^{2+} released from the ER was significantly ($P<0.05$, $N=7$) higher in A549 cells (Figure 4b), suggesting a reduced IP_3-sensitive pool in A549-T24.

ER calcium pools

When TG was added to the ATP pretreated cells in the presence of extracellular calcium, a rapid and robust increase in $[Ca^{2+}]_c$ was observed (Figure 5a and b), followed by a prolonged plateau in both cell lines. The addition of Ni^{2+} returned the calcium signals to the base level. However, in the absence of extracellular calcium, ATP pretreatment had different effects on TG-mediated $[Ca^{2+}]_{er}$ release. A 57% decrease in TG response was observed in ATP pretreated A549 cells, as determined by the fluorescence ratio, while no significant difference was seen in A549-T24 cells (Figure 5c). In contrast, the addition of ATP after TG resulted in almost complete inhibition of ATP response in both cell lines (Figure 5d).

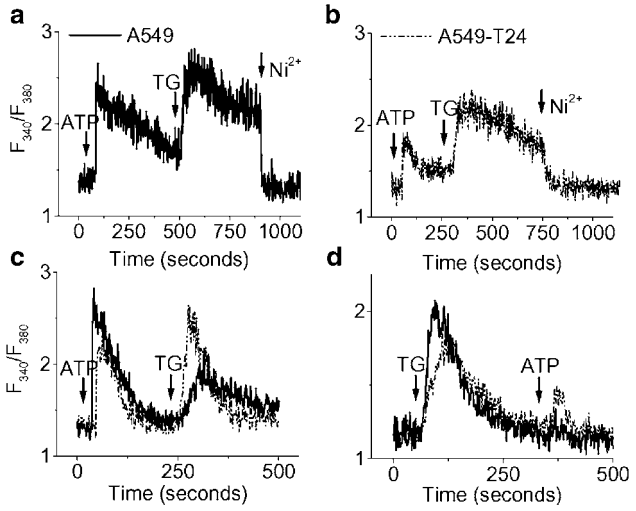

Figure 5 Effect of ATP pretreatment on TG-mediated Ca^{2+} signals. (a, b) A representative tracing of the response of $[Ca^{2+}]_i$ of A549 (a) and A549-T24 (b) cells in response to ATP (100 μM) in the presence of 1.2 mM $[Ca^{2+}]_o$, followed by TG (100 nM) treatment and Ni^{2+} (10 mM) treatment. (c, d) Representative traces of $[Ca^{2+}]_{er}$ release in A549 and A549-T24 cells in the absence of extracellular calcium. In (c), the cells were first treated with ATP (100 μM) followed by TG (100 nM). In (d), the order of addition of these agents was reversed.

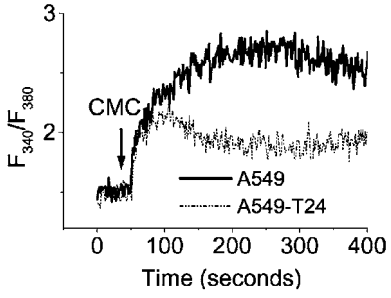

Figure 6 RyR-mediated Ca^{2+} release. Representative traces of the response of $[Ca^{2+}]_i$ of A549 and A549-T24 cells in response to CMC (500 μM) in the presence of 1.2 mM extracellular calcium.

Ryanodine receptor (RyR) agonist-mediated Ca^{2+} release

RyR are large integral membrane proteins that serve as major intracellular calcium release channels. A549 cells have been reported to express RyR (Xue *et al*., 2000). We used CMC, a potent pharmacological RyR agonist (Kiselyov *et al*., 2000), to study the RyR mediated calcium release in our cell lines. CMC (500 μM) induced a sustained increase in $[Ca^{2+}]_c$ in both cell lines in the presence of 1.2 mM extracellular Ca^{2+}. However, the amplitude of CMC-mediated elevation of $[Ca^{2+}]_c$ was 1.9-fold higher ($P<0.01$, $N=6$) in A549 cells than in A549-T24 cells, as judged by the fluorescence ratio at the plateau phase (Figure 6).

Analysis of SERCA expression

To determine the possible role of SERCA in altered $[Ca^{2+}]_{er}$, we studied the mRNA expression pattern of SERCA2b and

SERCA3 in our cell lines. A single band of the predicted size for SERCA2b and SERCA3 was detected in both A549 and A549-T24 cells (Figure 7). The expression level of 18S ribosomal RNA was used as an internal control to correct for inter-sample variations in total RNA abundance. SERCA2b mRNA was expressed in high levels in both cell lines (Figure 7). However, there was no difference in its expression level between the two cell lines. Furthermore, the mRNA expression of SERCA3 was very low with no difference between A549 and A549-T24 (Figure 7).

Analysis of Trp expression

To determine whether the reduced TG induced Ca^{2+} signals in A549-T24 cells are due to altered SOC expression, we analyzed Trp mRNA expression levels. Trp expression has been previously reported in A549 cells by Brough *et al.* (Brough *et al.*, 2001). We observed Trp1, Trp3 and Trp4 transcripts in both the cell lines (Figure 8). There were no differences in their expression levels between the two cell lines.

Analysis of sorcin and Bcl-2 expression

A single band of predicted size for sorcin (367 bp) was detected in both A549 and A549-T24 cells. As shown in Figure 9a, in comparison to A549 cells, A549-T24 cells expressed significantly higher levels (27%, $P<0.05$, $N=3$) of sorcin mRNA.

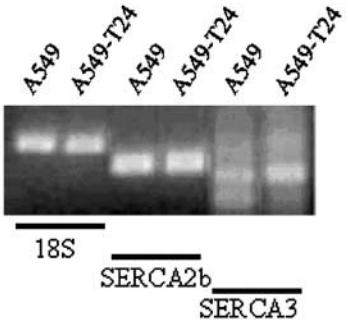

Figure 7 SERCA mRNA expression in A549 and A549-T24 cells. Semi-quantitative RT–PCR analysis of SERCA2b and SERCA3 were carried out using isoform-specific primers as described in Methods. The expression level of 18S ribosomal RNA served as an internal control.

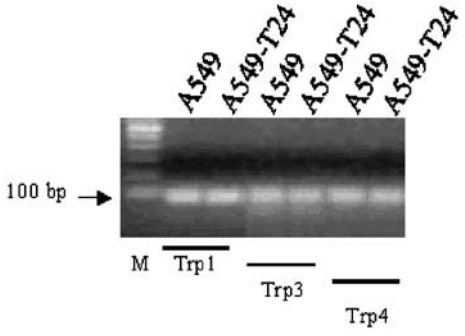

Figure 8 TRP mRNA expression in A549 and A549-T24 cells. Semi-quantitative RT–PCR analysis of Trp1, 3 and 4 was carried out as described in Methods. A 100-bp DNA ladder was used to estimate the size of the amplified products. M: 100 bp DNA ladder.

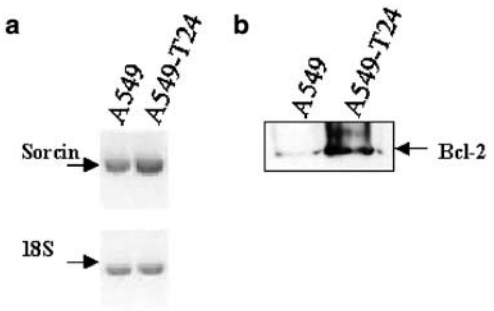

Figure 9 Expression of sorcin and Bcl-2 in A549 and A549-T24 cells. Semi-quantitative RT–PCR analysis of sorcin mRNA expression (a), and Western blot analysis of Bcl-2 (22 kDa) protein expression (b) were carried out as described in Methods. The intensities of the bands were measured by densitometry. The expression of 18S ribosomal RNA was used as an internal control. A549-T24 cells expressed significantly higher levels of sorcin mRNA ($P<0.05$, $N=3$), and Bcl-2 protein ($P<0.01$, $N=3$).

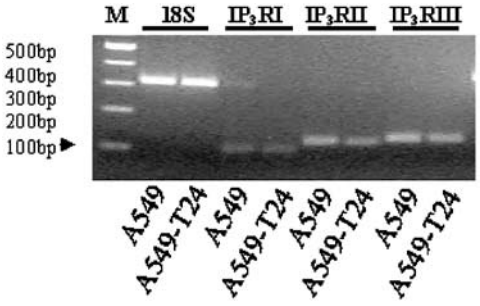

Figure 10 mRNA expression of IP_3R type I (IP_3RI), type II (IP_3RII) and type III (IP_3RIII) in A549 and A549-T24 cells. Semi-quantitative RT–PCR analysis of IP_3RI, IP_3RII and IP_3RIII were carried out as described in Methods. The expression of 18S ribosomal RNA was used as an internal control. A 100-bp DNA ladder was used to estimate the size of the amplified products. M: 100 bp DNA ladder.

Expression of Bcl-2 was negligible in A549 cells as determined by Western blot analysis (Figure 9b). In contrast, A549-T24 cells expressed significantly ($P<0.01$, $N=3$) higher levels of Bcl-2 (Figure 9b).

Analysis of IP_3 receptor expression

To determine whether the differential ATP response in the two cell lines is due to altered IP3 receptor expression, we analyzed mRNA expression of IP_3 receptor type I, II and III. As shown in Figure 10, both the cell lines expressed all three subtypes of IP_3 receptor. Densitometric analysis suggested that the mRNA was similar in both the cell lines. IP_3 receptor type II and III were expressed in much higher levels compared to IP_3 receptor type I.

Calcium signals after Taxol treatment

To investigate the changes in calcium homeostasis in tumor cells during Taxol-induced apoptosis, the cells were treated with IC_{50} concentrations of Taxol (20 nM in A549 and 200 nM in A549-T24) for 24 h. This time point was chosen to

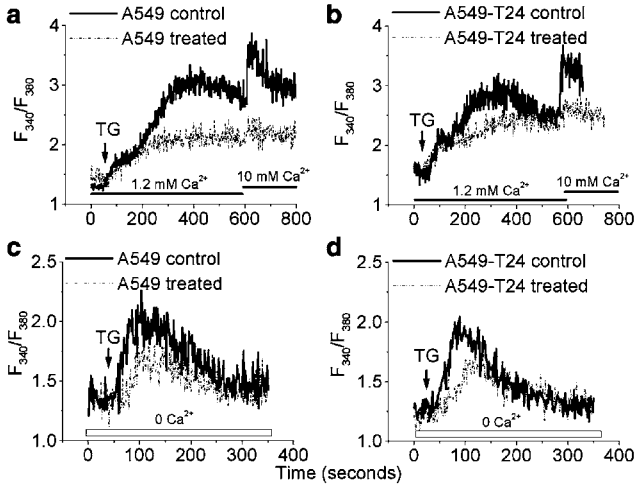

Figure 11 TG-evoked Ca^{2+} response in Taxol-treated cells. The tumor cells were treated with either vehicle (control, solid line) or IC_{50} concentrations of Taxol (treated, dotted line) for 24 h. $[Ca^{2+}]_c$ in Fura-2-AM-loaded cells were then measured as described in Methods. (a, b) A representative tracing of the response of $[Ca^{2+}]_i$ of A549 (a) and A549-T24 (b) cells in response to TG (100 nM) in the presence of 1.2 mM of calcium, followed by addition of extracellular calcium (10 mM). (c, d) A representative tracing of the response of $[Ca^{2+}]_i$ of A549 (c) and A549-T24 (d) cells in response to TG (100 nM) in the absence of extracellular calcium.

investigate the calcium changes prior to the onset of apoptosis. The effect of various Ca^{2+} releasing agents on intracellular Ca^{2+} was measured. As shown in Figure 11, Taxol treatment of A549 (Figure 11a) and A549-T24 (Figure 11b) reduced TG induced Ca^{2+} influx in the presence of 1.2 mM extracellular Ca^{2+}. Moreover, the addition of 10 mM Ca^{2+} to the extracellular medium did not result in increased $[Ca^{2+}]_c$. When stimulated with TG in the absence of extracellular Ca^{2+}, we observed a significant reduction in the Ca^{2+} signal in Taxol treated A549 (Figure 11c) and A549-T24 (Figure 11d) cells compared to the control cells. AUC calculations revealed a significant ($P<0.05$, $N=6$) decrease in TG-mediated $[Ca^{2+}]_{er}$ release in Taxol-treated A549 and A549-T24 cells.

Discussion

Our cytotoxicity studies revealed that A549-T24 cells are resistant to Taxol-induced apoptosis in that the IC_{50} of Taxol is 10 times higher in these cells compared to their parent cell line. Previous studies by Kavallaris *et al.* (1997) have shown that the altered expression of specific β-tubulin leads to decreased Taxol binding, thereby resulting in reduced sensitivity to the drug in A549-T24 cells. Clinically, chemoresistance is seldom due to a single mechanism. Therefore, it is important to understand the various resistance pathways so that more effective therapies can be designed.

Despite extensive studies on the role of calcium in cell death, the mechanisms linking impaired calcium homeostasis to chemoresistance are poorly understood. Here, we systematically analyzed various components of intracellular calcium homeostasis and their relative contribution to altered cellular calcium levels in drug-resistant tumor cells. A major finding in the current study is that altered ER calcium homeostasis is associated with resistance to Taxol-mediated apoptosis. We also found increased sorcin and Bcl-2 in the resistant cell line, an observation that may account for decreased responses to agonist-mediated ER calcium release.

TG is one of the most commonly used agents in pharmacological studies of Ca^{2+} stores (Thastrup *et al.*, 1990; Treiman *et al.*, 1998). Inhibition of SERCA pumps with TG caused an increase in $[Ca^{2+}]_c$ in both A549 and A549-T24 cells. The common cellular response to TG is biphasic with an initial peak followed by a somewhat lower plateau. In contrast, in the cancer cell lines used in this study, TG elicits a triphasic response characterized by an initial step increase, which at a critical 'notch' value is followed by the classical two phases of peak and plateau. This unique 'triphasic' response may be attributed to a delay in the generation of signal(s) activating Ca^{2+} influx. Since the magnitude of the first plateau (Figure 3c) is similar to the response seen in the absence of extracellular Ca^{2+} (Figure 3g), it can be concluded that the first phase is mainly due to Ca^{2+} release from the ER. In addition, the fact that the second and third phases appear only in the presence of extracellular Ca^{2+} suggests that they are due to Ca^{2+} influx. The factors contributing to this delay in Ca^{2+} entry are currently unknown, but may be related to the time required for sufficient ER depletion to occur before initiation of CCE. In the current study, we found that the basal levels of $[Ca^{2+}]_c$ were similar in A549 and A549-T24 cells. However, the TG-induced calcium response profiles were dramatically different. TG induced a much smaller increase in cytosolic Ca^{2+} levels, with both reduced release and influx components in A549-T24 cells. ER store depletion under physiological conditions typically results in a large increase in $[Ca^{2+}]_c$ due to Ca^{2+} influx through SOC, which serves to refill the Ca^{2+} stores (Putney, 1986; Putney *et al.*, 2001). The sensitivity of TG- and ATP-induced responses to SK&F96365 and Ni^{2+} strongly suggests that Ca^{2+} influx is through SOC and possibly by ROC-type channels. Further, our data suggest that the reduced Ca^{2+} influx response in A549-T24 cells represents a real attenuation of SOC activity compared to A549 cells. Indeed, the reduced $[Ca^{2+}]_c$ response in the A549-T24 cells is most likely not due to hyperactive Ca^{2+} extrusion processes given that we did not observe significant differences in the $[Ca^{2+}]_c$ decline rates, but did see greater Ba^{2+} influx in TG-stimulated A549 cells as compared to A549-T24 cells. Ba^{2+} enters the cells through nonselective cation channels and is not extruded by pumps/exchanger as efficiently as Ca^{2+}, enabling a unidirectional assessment of divalent cation flow based on the assumption that cation selectivity of the channel has not changed.

Trp1 is known to encode a component of SOC (Liu *et al.*, 2000). We showed the mRNA expression of Trp1, 3 and 4 in A549 cells, which is in agreement with the previously published data (Xue *et al.*, 2000; Brough *et al.*, 2001). Since we did not find a significant difference in the mRNA expression of these channels between the two cell lines, this suggests that the reduced Ca^{2+} entry in the chemoresistant cell line may not be due to altered Trp mRNA expression.

Maintenance of ER calcium ($[Ca^{2+}]_{er}$) homeostasis plays a pivotal role in various cellular processes such as cell growth, division and protein processing (Berridge *et al.*, 2000). Consequently, both $[Ca^{2+}]_{er}$ overload and abnormal Ca^{2+} discharge from the ER are potential precipitating factors in the activation of cell death pathways. Two major pathways of

Ca^{2+} release from the ER are mediated by IP_3R and RyR. Although the two cell lines expressed similar levels of IP_3 receptors, their calcium release profiles in response to IP_3R agonists were dramatically different. An important finding in the present work is that A549-T24 cells had not only reduced IP_3 and ryanodine-sensitive pools, as judged by ATP and CMC responses, but also the TG releasable $[Ca^{2+}]_{er}$ was significantly reduced. This is significant in view of the previously known association between the reduced ER calcium and protection against apoptosis (Ferrari *et al*., 2002).

An additional notable difference in A549 and A549-T24 responses is the kinetics of Ca^{2+} signals upon ATP stimulation. What stands out most is the rapid decline in the initial phase of the calcium influx, followed by a prolonged plateau. This peculiar feature in these cells could be due to one or more of the following reasons: (i) reduced function of SOC, (ii) faster reuptake of Ca^{2+} by ER, (iii) increased efflux of Ca^{2+} through PMCA (plasma membrane Ca^{2+}-ATPase) or NCX (Na^+/Ca^{2+} exchanger) and (iv) inefficient coupling of store depletion to SOC. As we reported before (Nazer & Van Breemen, 1998), removal of Ca^{2+} from the extracellular space in the presence of a SERCA inhibitor allows measurement of the decay in $[Ca^{2+}]_i$ as a function of Ca^{2+} extrusion. Our previous results indicated that in the absence of extracellular Ca^{2+} little refilling occurs, so that the decay in $[Ca^{2+}]_i$ referred to above is an estimate of Ca^{2+} extrusion. The observation that this rate of $[Ca^{2+}]_i$ decline upon removal of extracellular Ca^{2+} in the presence of TG was similar in both cell lines suggests that the Ca^{2+} removal processes are the same for both cell lines. Furthermore, the addition of 3 mM La^{3+} returned the calcium signals to the baseline with no difference in Ca^{2+} decay in A549 and A549-T24 cells. This may also indicate that the Ca^{2+} removal processes are the same for both cell lines (Figure 3e). The observation that the effect of La^{3+} was very similar to the effect of external Ca^{2+} removal suggests that the effect of La^{3+} was due to inhibition of Ca^{2+} influx. Since La^{3+} is also known to inhibit Ca^{2+} extrusion, a contribution by organellar Ca^{2+} uptake appears likely. In this respect, it is interesting to note that inhibition of ER uptake with TG or mitochondrial Ca^{2+} uptake with CCCP led in both cases to a large Ca^{2+} release transient. The mitochondrial and ER Ca^{2+} stores appeared to be separate in so far that the CCCP-induced Ca^{2+} release did not affect a subsequent release stimulated by TG (data not shown). Furthermore, the fact that we were able to observe a $[Ca^{2+}]_i$ transient after application of La^{3+} suggests that the Fura-2 was not quenched.

Interestingly, the TG-induced Ca^{2+} response was altered by the ATP pretreatment in that there is an immediate rise in $[Ca^{2+}]_c$. A possible reason for the abolition of the delay in Ca^{2+} influx is that the ATP-mediated store depletion has already resulted in the opening of the SOC channels. Inhibition of SERCA with TG would prevent recycling of Ca^{2+} between IP_3R and SERCA, thus increasing the effectiveness of Ca^{2+} influx through SOC in raising $[Ca^{2+}]_i$. Although in the current study both cell lines exhibited a similar overall Ca^{2+} mobilization pattern in terms of the rise in $[Ca^{2+}]_c$ and sustained influx, the amplitude of the TG effect was still less in the resistant cell line. In the absence of extracellular Ca^{2+}, however, the amount of Ca^{2+} released by TG was significantly reduced by ATP pretreatment compared to TG treatment alone in A549 cells. In contrast, ATP pretreatment had no significant effect on TG responses in A549-T24 cells as TG released similar amounts of Ca^{2+} with or without ATP pretreatment. When the above agents were added in reverse order, TG completely abolished the effect of ATP. Taken together, these data (Figure 5a-d) suggest the presence of two pools, a TG- and ATP-sensitive pool, and a pool exclusively sensitive to TG. The ATP-sensitive pool is probably smaller in the resistant cell line than that present in the parent cell line. Therefore, one cannot see the difference in TG-induced calcium release after ATP application in T549-24. To test this possibility, the cells were treated with other IP_3-linked agonists bradykinin (1 μM) and histamine (50 μM), and $[Ca^{2+}]_c$ was measured (data not shown). Reduced responses to these agents in the chemoresistant cell line further suggested reduced IP_3-sensitive pools in A549-T24 cells. Further investigation is required to determine the relative importance of these findings in chemoresistance.

Uptake of calcium into the ER is mediated by SERCA. Among three different isoforms (SERCA1, 2 and 3), SERCA2b is ubiquitously expressed in all non-muscle cells. SERCA3 is coexpressed with SERCA2 in several non-muscle cells. SERCA expression has been shown to be regulated by cytosolic calcium levels (Wu *et al*., 2001; Liu *et al*., 2002). The level of SERCA2b expression and activity closely correlated with ER Ca^{2+} content and growth rate in LNCaP cells (Legrand *et al*., 2001). In contrast, overexpression of SERCA2b by gene transfer in COS cells induced endosarcoplasmic reticulum Ca^{2+} overload, resulting in apoptosis (Ma *et al*., 1999). Our observation that SERCA2b and SERCA3 mRNA are expressed at similar levels suggests that the differential ER calcium content in our cell lines is not due to altered SERCA mRNA expression. However, altered SERCA activity cannot be ruled out.

It is becoming increasingly evident that the Bcl-2 oncogene, the expression of which may lead to tumor growth and often chemoresistance, has a direct effect on ER Ca^{2+} handling (Granville *et al*., 2001; Ferrari *et al*., 2002; Pinton *et al*., 2002). Acting as an ion channel, it increases the passive leak of Ca^{2+} from ER, thereby decreasing the steady-state $[Ca^{2+}]_{er}$. In addition, it downregulates the capacitative current by modulating SOC activity.

Furthermore, *in vitro* transfection studies have provided direct evidence in support of the protective role of Bcl-2 against C2-ceramide or TNF-induced apoptosis through its ability to decrease the releasable Ca^{2+} pool in the ER (Pinton *et al*., 2001; Kim *et al*., 2002). In the present study, the finding that Bcl-2 protein is significantly elevated in A549-T24 cells suggests its possible role in reduced $[Ca^{2+}]_{er}$.

There is also an emerging interest in the role of sorcin in chemoresistance. Sorcin can bind and thereby sequester up to 10% of the cytosolic calcium. In addition, this cytosolic protein translocates to the ER membrane during RyR-mediated Ca^{2+} release. The binding of sorcin to RyR results in receptor blockade (Lokuta *et al*., 1997). In the present study, we found higher levels of sorcin mRNA in A549-T24 cells compared to the parent cell line. Increased sorcin may be partially responsible for the reduced effect of CMC in A549-T24 cells by blocking the RyR-mediated Ca^{2+} release from the ER. Taken together, the reduced ER content may contribute to the decreased sensitivity to drug-mediated apoptosis, leading to the development of chemoresistance.

It has been recently suggested (Srivastava *et al*., 1999) that Taxol induces apoptosis at least in part through the induction

of FasL, the transcription of which depends on nuclear factor of activated T lymphocytes (NFAT). The activation of NFAT strictly depends on calcineurin, which in turn requires Ca^{2+} released from IP_3 releasable pools. Inhibition of the calcineurin-NFAT-FasL pathway has been shown to confer Taxol resistance in tumor cells (Srivastava *et al*., 1999; Biswas *et al*., 2001). Therefore, it is tempting to speculate that this calcium pathway is defective in A549-T24 cells.

Kidd *et al*. (2002) have shown that Taxol can increase cytosolic Ca^{2+} levels by damaging the mitochondria. In contrast, Taxol has been shown to inhibit Ca^{2+} entry in several cell types through its ability to stabilize microtubules (Burke *et al*., 1994; Furukawa & Mattson, 1995). Interestingly, 24 h Taxol treatment resulted in a significant decrease in Ca^{2+} influx following TG application in our experimental model. Of particular interest is the decreased SOC function in A549-T24 compared to A549 in the absence of Taxol. The fact that these cells survive with depressed SOC function may suggest that they may have developed compensatory mechanism(s) to accommodate the defect of SOC. Another interesting finding was the absence of a rapid increase in $[Ca^{2+}]_c$ upon the addition of supra-physiological levels of Ca^{2+} to the extracellular media. These data suggest an altered Ca^{2+} influx mechanism in Taxol-damaged cells. In addition, TG treatment in the absence of extracellular Ca^{2+} revealed a reduced ER Ca^{2+} pool in Taxol treated cells. This could be due to either reduced refilling of ER (as a result of defective Ca^{2+} influx) and/or increased leakiness of ER Ca^{2+} channels (due to damage to the ER). A sudden release of large amounts of calcium that is not compensated by refilling can be damaging to cells. The A549-T24 cell line may be partially resistant to this damage, as it has developed adaptive changes in ER calcium-handling mechanisms (such as reduced $[Ca^{2+}]_{er}$ levels as well as Ca^{2+} release upon stimulation).

In contrast to the TG responses, no significant difference was observed between the control and Taxol-treated groups in terms of ATP responses (data not shown). Similar observations have been reported in other cell types (Hamm-Alvarez *et al*., 1994). The apparent discrepancy with respect to ATP and TG responses could arise from several factors. First, signals that couple ATP- and TG-mediated store depletion and their regulation may be different in the two cell lines. In the case of TG, these signals (such as conformational coupling or vesicle transport) may depend on an intact cytoskeleton. Taxol, by damaging the microtubules, may selectively inhibit the signals activated by TG treatment. Second, as previously proposed (Bennett *et al*., 1998; Venkatachalam *et al*., 2002), TG- and ATP-evoked CCE pathways may be different due to their ability to activate distinct plasma membrane channels.

In summary, the present work revealed a number of interesting observations regarding the modulation of intracellular calcium homeostasis accompanying the development of chemoresistance in NSCLC cells. However, this study represents the analysis of a single clone (A549-T24 selected for Taxol resistance) compared with the wild-type population of A549 cells. Analysis of the variation in Ca^{2+} signaling properties between clonal samples within the parental population may allow an estimate of the degree of difference between these wild-type clones unselected for chemoresistance and the A549-T24 clone studied here. Further studies on additional Taxol-resistant clones will also permit a better assessment of clonal variation in the parameters conferring resistance. In addition, how these findings relate to mechanisms of Taxol resistance must be further investigated.

This work was supported by the National Heart, Lung, and Blood Institute Grant R15HL071520. We thank Dr Paul Richmond, Department of Biology, and Dr William Chan, Department of Pharmaceutics and Medicinal Chemistry, the University of the Pacific, for their kind support and providing equipment for the fluorescence microscopy and RT–PCR assay.

References

BENNETT, D.L., BOOTMAN, M.D., BERRIDGE, M.J. & CHEEK, T.R. (1998). Ca^{2+} entry into PC12 cells initiated by ryanodine receptors or inositol 1,4,5-trisphosphate receptors. *Biochem. J.,* **329,** 349–357.

BERRIDGE, M.J., LIPP, P. & BOOTMAN, M.D. (2000). The versatility and universality of calcium signalling. *Nat. Rev. Mol. Cell. Biol.,* **1,** 11–21.

BISWAS, R.S., CHA, H.J., HARDWICK, J.M. & SRIVASTAVA, R.K. (2001). Inhibition of drug-induced Fas ligand transcription and apoptosis by Bcl-XL. *Mol. Cell Biochem.,* **225,** 7–20.

BLAGOSKLONNY, M.V. & FOJO, T. (1999). Molecular effects of paclitaxel: myths and reality (a critical review). *Int. J. Cancer,* **83,** 151–156.

BROUGH, G.H., WU, S., CIOFFI, D., MOORE, T.M., LI, M., DEAN, N. & STEVENS, T. (2001). Contribution of endogenously expressed Trp1 to a Ca^{2+}-selective, store-operated Ca^{2+} entry pathway. *Faseb. J.,* **15,** 1727–1738.

BROWNLOW, S.L. & SAGE, S.O. (2003). Rapid agonist-evoked coupling of type II Ins(1,4,5)P3 receptor with human transient receptor potential (hTRPC1) channels in human platelets. *Biochem. J.,* **375,** 697–704.

BURKE, W.J., RAGHU, G. & STRONG, R. (1994). Taxol protects against calcium-mediated death of differentiated rat pheochromocytoma cells. *Life Sci.,* **55,** 313–319.

CHEN, J.S., AGARWAL, N. & MEHTA, K. (2002). Multidrug-resistant MCF-7 breast cancer cells contain deficient intracellular calcium pools. *Breast Cancer Res. Treat.,* **71,** 237–247.

FERRARI, D., PINTON, P., SZABADKAI, G., CHAMI, M., CAMPANELLA, M., POZZAN, T. & RIZZUTO, R. (2002). Endoplasmic reticulum, Bcl-2 and Ca(2+) handling in apoptosis. *Cell Calcium,* **32,** 413–420.

FERRY, D.R., TRAUNECKER, H. & KERR, D.J. (1996). Clinical trials of P-glycoprotein reversal in solid tumours. *Eur. J. Cancer,* **32A,** 1070–1081.

FURUKAWA, K. & MATTSON, M.P. (1995). Taxol stabilizes $[Ca^{2+}]_i$ and protects hippocampal neurons against excitotoxicity. *Brain Res.,* **689,** 141–146.

GRAF, E., VERMA, A.K., GORSKI, J.P., LOPASCHUK, G., NIGGLI, V., ZURINI, M., CARAFOLI, E. & PENNISTON, J.T. (1982). Molecular properties of calcium-pumping ATPase from human erythrocytes. *Biochemistry,* **21,** 4511–4516.

GRANVILLE, D.J., RUEHLMANN, D.O., CHOY, J.C., CASSIDY, B.A., HUNT, D.W., VAN BREEMEN, C. & MCMANUS, B.M. (2001). Bcl-2 increases emptying of endoplasmic reticulum Ca^{2+} stores during photodynamic therapy-induced apoptosis. *Cell Calcium,* **30,** 343–350.

GRYNKIEWICZ, G., POENIE, M. & TSIEN, R.Y. (1985). A new generation of Ca^{2+} indicators with greatly improved fluorescence properties. *J. Biol. Chem.,* **260,** 3440–3450.

HAMM-ALVAREZ, S.F., ALAYOF, B.E., HIMMEL, H.M., KIM, P.Y., CREWS, A.L., STRAUSS, H.C. & SHEETZ, M.P. (1994). Coordinate depression of bradykinin receptor recycling and microtubule-dependent transport by taxol. *Proc. Natl. Acad. Sci. U.S.A.,* **91,** 7812–7816.

KALIVENDI, S.V., KOTAMRAJU, S., ZHAO, H., JOSEPH, J. & KALYANARAMAN, B. (2001). Doxorubicin-induced apoptosis is associated with increased transcription of endothelial nitric-oxide synthase. Effect of antiapoptotic antioxidants and calcium. *J. Biol. Chem.,* **276,** 47266–47276.

KAVALLARIS, M., KUO, D.Y., BURKHART, C.A., REGL, D.L., NORRIS, M.D., HABER, M. & HORWITZ, S.B. (1997). Taxol-resistant epithelial ovarian tumors are associated with altered expression of specific beta-tubulin isotypes. *J. Clin. Invest.,* **100,** 1282–1293.

KAWANO, S., SHOJI, S., ICHINOSE, S., YAMAGATA, K., TAGAMI, M. & HIRAOKA, M. (2002). Characterization of Ca(2+) signaling pathways in human mesenchymal stem cells. *Cell Calcium,* **32,** 165–174.

KIDD, J.F., PILKINGTON, M.F., SCHELL, M.J., FOGARTY, K.E., SKEPPER, J.N., TAYLOR, C.W. & THORN, P. (2002). Paclitaxel affects cytosolic calcium signals by opening the mitochondrial permeability transition pore. *J. Biol. Chem.,* **277,** 6504–6510.

KIM, B.C., KIM, H.T., MAMURA, M., AMBUDKAR, I.S., CHOI, K.S. & KIM, S.J. (2002). Tumor necrosis factor induces apoptosis in hepatoma cells by increasing Ca(2+) release from the endoplasmic reticulum and suppressing Bcl-2 expression. *J. Biol. Chem.,* **277,** 31381–31389.

KISELYOV, K.I., SHIN, D.M., WANG, Y., PESSAH, I.N., ALLEN, P.D. & MUALLEM, S. (2000). Gating of store-operated channels by conformational coupling to ryanodine receptors. *Mol. Cell,* **6,** 421–431.

LEGRAND, G., HUMEZ, S., SLOMIANNY, C., DEWAILLY, E., VANDEN ABEELE, F., MARIOT, P., WUYTACK, F. & PREVARSKAYA, N. (2001). Ca^{2+} pools and cell growth. Evidence for sarcoendoplasmic Ca^{2+}-ATPases 2B involvement in human prostate cancer cell growth control. *J. Biol. Chem.,* **276,** 47608–47614.

LI, G., TAN, Y., YANG, C., ZHAO, C., ZHAO, H., WANG, J., XUE, Y., HAN, M. & QIAN, L. (2002). Expression and clinical implication of soluble resistance-associated calcium-binding protein gene and multi-drug resistance gene in leukemia. *Zhonghua Zhong Liu Za Zhi,* **24,** 370–374.

LIANG, X. & HUANG, Y. (2000). Intracellular free calcium concentration and cisplatin resistance in human lung adenocarcinoma A549 cells. *Biosci. Rep.,* **20,** 129–138.

LIU, L., PATERSON, C.A. & BORCHMAN, D. (2002). Regulation of sarco/endoplasmic Ca^{2+}-ATPase expression by calcium in human lens cells. *Exp. Eye Res.,* **75,** 583–590.

LIU, X., WANG, W., SINGH, B.B., LOCKWICH, T., JADLOWIEC, J., O'CONNELL, B., WELLNER, R., ZHU, M.X. & AMBUDKAR, I.S. (2000). Trp1, a candidate protein for the store-operated Ca(2+) influx mechanism in salivary gland cells. *J. Biol. Chem.,* **275,** 3403–3411.

LOKUTA, A.J., MEYERS, M.B., SANDER, P.R., FISHMAN, G.I. & VALDIVIA, H.H. (1997). Modulation of cardiac ryanodine receptors by sorcin. *J. Biol. Chem.,* **272,** 25333–25338.

LYNCH, K., FERNANDEZ, G., PAPPALARDO, A. & PELUSO, J.J. (2000). Basic fibroblast growth factor inhibits apoptosis of spontaneously immortalized granulosa cells by regulating intracellular free calcium levels through a protein kinase C delta-dependent pathway. *Endocrinology,* **141,** 4209–4217.

MA, T.S., MANN, D.L., LEE, J.H. & GALLINGHOUSE, G.J. (1999). SR compartment calcium and cell apoptosis in SERCA overexpression. *Cell Calcium,* **26,** 25–36.

MAKI, M., KITAURA, Y., SATOH, H., OHKOUCHI, S. & SHIBATA, H. (2002). Structures, functions and molecular evolution of the penta-EF-hand Ca^{2+}-binding proteins. *Biochim. Biophys. Acta.,* **1600,** 51–60.

MANDIC, A., HANSSON, J., LINDER, S. & SHOSHAN, M.C. (2002). Cisplatin induces ER stress and nucleus-independent apoptotic signaling. *J. Biol. Chem.,* **31,** 31.

MARIN, M.C., FERNANDEZ, A., BICK, R.J., BRISBAY, S., BUJA, L.M., SNUGGS, M., MCCONKEY, D.J., VON ESCHENBACH, A.C., KEATING, M.J. & MCDONNELL, T.J. (1996). Apoptosis suppression by bcl-2 is correlated with the regulation of nuclear and cytosolic Ca^{2+}. *Oncogene,* **12,** 2259–2266.

MCCONKEY, D.J. (1996). The role of calcium in the regulation of apoptosis. *Scanning Microsc.,* **10,** 777–793.

MCCONKEY, D.J., NICOTERA, P., HARTZELL, P., BELLOMO, G., WYLLIE, A.H. & ORRENIUS, S. (1989). Glucocorticoids activate a suicide process in thymocytes through an elevation of cytosolic Ca^{2+} concentration. *Arch. Biochem. Biophys.,* **269,** 365–370.

MESTDAGH, N., VANDEWALLE, B., HORNEZ, L. & HENICHART, J.P. (1994). Comparative study of intracellular calcium and adenosine 3′,5′-cyclic monophosphate levels in human breast carcinoma cells sensitive or resistant to adriamycin: contribution to reversion of chemoresistance. *Biochem. Pharmacol.,* **48,** 709–716.

MILLER, M.L. & OJIMA, I. (2001). Chemistry and chemical biology of taxane anticancer agents. *Chem. Rec.,* **1,** 195–211.

NAZER, M.A. & VAN BREEMEN, C. (1998). A role for the sarcoplasmic reticulum in Ca^{2+} extrusion from rabbit inferior vena cava smooth muscle. *Am. J. Physiol.,* **274,** H123–H131.

NYGREN, P., LARSSON, R., GRUBER, A., PETERSON, C. & BERGH, J. (1991). Doxorubicin selected multidrug-resistant small cell lung cancer cell lines characterised by elevated cytoplasmic Ca^{2+} and resistance modulation by verapamil in absence of P-glycoprotein overexpression. *Br. J. Cancer,* **64,** 1011–1018.

PAREKH, H.K., DENG, H.B., CHOUDHARY, K., HOUSER, S.R. & SIMPKINS, H. (2002). Overexpression of sorcin, a calcium-binding protein, induces a low level of paclitaxel resistance in human ovarian and breast cancer cells. *Biochem. Pharmacol.,* **63,** 1149–1158.

PINTON, P., FERRARI, D., RAPIZZI, E., DI VIRGILIO, F., POZZAN, T. & RIZZUTO, R. (2002). A role for calcium in Bcl-2 action? *Biochimie.,* **84,** 195–201.

PINTON, P., FERRARI, D., RAPIZZI, E., DI VIRGILIO, F.D., POZZAN, T. & RIZZUTO, R. (2001). The Ca^{2+} concentration of the endoplasmic reticulum is a key determinant of ceramide-induced apoptosis: significance for the molecular mechanism of Bcl-2 action. *EMBO J.,* **20,** 2690–2701.

PUTNEY JR, J.W. (1986). A model for receptor-regulated calcium entry. *Cell Calcium,* **7,** 1–12.

PUTNEY JR, J.W., BROAD, L.M., BRAUN, F.J., LIEVREMONT, J.P. & BIRD, G.S. (2001). Mechanisms of capacitative calcium entry. *J. Cell Sci.,* **114,** 2223–2229.

RICCIO, A., MEDHURST, A.D., MATTEI, C., KELSELL, R.E., CALVER, A.R., RANDALL, A.D., BENHAM, C.D. & PANGALOS, M.N. (2002). mRNA distribution analysis of human TRPC family in CNS and peripheral tissues. *Brain. Res. Mol. Brain Res.,* **109,** 95–104.

SRIVASTAVA, R.K., SASAKI, C.Y., HARDWICK, J.M. & LONGO, D.L. (1999). Bcl-2-mediated drug resistance: inhibition of apoptosis by blocking nuclear factor of activated T lymphocytes (NFAT)-induced Fas ligand transcription. *J. Exp. Med.,* **190,** 253–265.

TAN, Y., LI, G., ZHAO, C., WANG, J., ZHAO, H., XUE, Y., HAN, M. & YANG, C. (2003). Expression of sorcin predicts poor outcome in acute myeloid leukemia. *Leuk. Res.,* **27,** 125–131.

THASTRUP, O., CULLEN, P.J., DROBAK, B.K., HANLEY, M.R. & DAWSON, A.P. (1990). Thapsigargin, a tumor promoter, discharges intracellular Ca^{2+} stores by specific inhibition of the endoplasmic reticulum Ca2(+)-ATPase. *Proc. Natl. Acad. Sci. U.S.A.,* **87,** 2466–2470.

TORRES, K. & HORWITZ, S.B. (1998). Mechanisms of Taxol-induced cell death are concentration dependent. *Cancer Res.,* **58,** 3620–3626.

TREIMAN, M., CASPERSEN, C. & CHRISTENSEN, S.B. (1998). A tool coming of age: thapsigargin as an inhibitor of sarco-endoplasmic reticulum Ca(2+)-ATPases. *Trends. Pharmacol. Sci.,* **19,** 131–135.

TRUMP, B.F. & BEREZESKY, I.K. (1995). Calcium-mediated cell injury and cell death. *FASEB J.,* **9,** 219–228.

TSURUO, T., IIDA, H., KAWABATA, H., TSUKAGOSHI, S. & SAKURAI, Y. (1984). High calcium content of pleiotropic drug-resistant P388 and K562 leukemia and Chinese hamster ovary cells. *Cancer Res.,* **44,** 5095–5099.

VALDIVIA, H.H. (1998). Modulation of intracellular Ca^{2+} levels in the heart by sorcin and FKBP12, two accessory proteins of ryanodine receptors. *Trends Pharmacol. Sci.,* **19,** 479–482.

VAN BREEMEN, C. & SAIDA, K. (1989). Cellular mechanisms regulating $[Ca^{2+}]_i$ smooth muscle. *Annu. Rev. Physiol.,* **51,** 315–329.

VENKATACHALAM, K., VAN ROSSUM, D.B., PATTERSON, R.L., MA, H.T. & GILL, D.L. (2002). The cellular and molecular basis of store-operated calcium entry. *Nat. Cell Biol.,* **4,** E263–E272.

WITKOWSKI, J.M. & MILLER, R.A. (1999). Calcium signal abnormalities in murine T lymphocytes that express the multidrug transporter P-glycoprotein. *Mech. Ageing Dev.,* **107,** 165–180.

WU, K.D., BUNGARD, D. & LYTTON, J. (2001). Regulation of SERCA Ca^{2+} pump expression by cytoplasmic Ca^{2+} in vascular smooth muscle cells. *Am. J. Physiol Cell Physiol.,* **280,** C843–C851.

XUE, H.H., ZHAO, D.M., SUDA, T., UCHIDA, C., ODA, T., CHIDA, K., ICHIYAMA, A. & NAKAMURA, H. (2000). Store depletion by caffeine/ryanodine activates capacitative Ca(2+) entry in nonexcitable A549 cells. *J. Biochem. (Tokyo),* **128,** 329–336.

(Received December 22, 2003
Revised February 15, 2004
Accepted February 23, 2004)